

ON THE SPIN HISTORY OF THE X-RAY PULSAR IN KES 73: FURTHER EVIDENCE FOR AN UTRAMAGNETIZED NEUTRON STAR

E. V. GOTTHELF¹, G. VASISHT², & T. DOTANI³

Draft version September 11, 2018

ABSTRACT

In previous papers, we presented the discovery of a 12-s X-ray pulsar in the supernova remnant Kes 73 providing the first direct evidence for an ultramagnetized neutron star, a magnetar, with an equivalent dipole field of nearly twenty times the quantum critical magnetic field ($m_e^2 c^3 / e\hbar$). Our conclusions were based on two epochs of measurement of the spin, along with an age estimate of the host supernova remnant. Herein, we present a spin chronology of the pulsar using additional *Ginga*, *ASCA*, *RXTE*, & *BeppoSAX* datasets spanning over a decade. Timing and spectral analysis confirms our initial results and severely limit an accretion origin for the observed flux. Over the 10 year baseline, the pulsar is found to undergo a rapid, constant spindown, while maintaining a steady flux and an invariant pulse profile. Within the measurement uncertainties, no systematic departures from a linear spin-down are found - departures as in the case of glitches or simply stochastic fluctuations in the pulse times-of-arrival (e.g. red timing noise). We suggest that this pulsar is akin to the soft γ -ray repeaters, however, it is remarkably stable and has yet to display similar outbursts; future γ -ray activity from this object is likely.

Subject headings: stars: individual (Kes 73, 1E 1841–045) — stars: neutron — supernova remnants — X-rays: stars

1. INTRODUCTION

The discovery of 12-s pulsed X-ray emission from the compact source within Kes 73 (Vasisht & Gotthelf 1997; herein VG97, Gotthelf & Vasisht 1997) came somewhat as a surprise, as this Einstein source (1E 1841–045) had been studied for some time (Kriss et al. 1985; Helfand et al. 1994). The pulsar was initially detected in an archived *ASCA* observation (1993) of Kes 73 (also SNR G27.4+0), and soon confirmed in an archived *ROSAT* dataset. The measured spindown from these detections indicated rapid braking on a timescale of $\tau_s \simeq 4 \times 10^3$ yr, consistent with the inferred age of the supernova remnant. The similarity in age along with the geometric location of the pulsar in the center of the symmetric and well defined remnant strongly suggests that the two objects are related.

There is sufficient evidence to argue that the host supernova remnant Kes 73 is relatively young, at age $\sim 2 \times 10^3$ yr (Helfand et al. 1994; Gotthelf & Vasisht 1997). Morphologically, it resembles any classic, limb-brightened shell-type radio supernova remnant, $\sim 4'$ in diameter, located at an HI derived distance of 6.0 – 7.5 kpc (Sanbonmatsu & Helfand 1992). Its diffuse X-ray emission is distributed throughout the remnant and has a spectrum characteristic of a hot plasma, $kT \simeq 0.8$ keV, along with fluorescence lines of several atomic species, including O-group elements, that indicate a young blast-wave of Type II or Ib origin, still rich in stellar ejecta. The relative abundance of ionized species of Si and S observed in the Kes 73 spectrum, suggest a level of ionization in-equilibrium consistent with an age $\lesssim 2 \times 10^3$ yr.

Based on the observed characteristics of Kes 73 and its X-ray pulsar, we suggested (VG97) that 1E 1841–045 was similar to the ‘anomalous’ X-ray pulsars (Mereghetti &

Stella 1995; van Paradijs, Taam & van den Heuvel 1995). We argued that 1E 1841–045 could not be an accreting neutron star; this was based on evolutionary arguments and the relative youth of Kes 73 and the fact that we found no evidence for accretion in our datasets. Instead, it was proposed that the X-ray pulsar was powered by an ultramagnetized neutron star with a dipole field of $B_s \simeq 7 \times 10^{14}$ G, and was the first of its kind; magnetic braking was assumed to be the predominant spindown mechanism, with $B_s \propto (P\dot{P})^{1/2}$. Since then, large magnetic fields have also been inferred for the soft γ -ray repeaters 1806–20 and 1900+14 (see Kouveliotou et al. 1998, 1999) via measurement of their spins and spindown with *RXTE* and *ASCA*.

In this paper we present a longterm spin history of the X-ray pulsar. We reinforce our original *ASCA* and *ROSAT* datasets with new *ASCA*, *RXTE*, & *BeppoSAX* pointings and ten year-old *Ginga* archival datasets, bringing the total number of timing observations of Kes 73 to seven. We show that the spin evolution obeys a steady linear spindown at a rate consistent, within errors, with our original estimate; re-affirming our somewhat marginal *ROSAT* detection (VG97).

2. OBSERVATIONS

2.1. *ASCA* & *BeppoSAX* Datasets

Kes 73 was re-observed with *ASCA* (Tanaka et al. 1994) on March 27–28, 1998, using an observing plan identical with the original 1993 observations. A complete description of the observing modes can be found in VG97. Here we concentrate on the high temporal resolution data (62 μ s or 48.8 ms depending on data mode) acquired with the two Gas Imaging Spectrometers (GIS2 & GIS3) on-board

¹Columbia Astrophysics Laboratory, Columbia University, 550 West 120th Street, New York, NY 10027, USA; evg@astro.columbia.edu

²Jet Propulsion Laboratory, California Institute of Technology, 4800 Oak Grove Drive, Pasadena, CA, 91109, USA; gv@astro.caltech.edu

³Institute of Space and Astronautical Science, 3-1-1 Yoshinodai, Sagamihara, Kanagawa 229, Japan; dotani@astro.isas.ac.jp

ASCA. The datasets was edited using the standard Rev 2 screening criteria which resulted in an effective exposure time of 39 ks per GIS sensor. Photons from the two GISs were merged and arrival times corrected to the barycenter. A log of all observations presented herein are given in Table 1.

We also acquired a 1.5 day *BeppoSAX* observation of Kes 73 on March 8-9, 1999 using the three operational narrow field instruments, the Low Energy Concentrator (LECS) and two Medium Energy Concentrators (MECS2 & MECS3). These imaging gas scintillation counters are similar to the GIS detectors, providing arcminute imaging over a $\sim 40'$ field-of-view in a broad energy band-pass of 0.1 – 12 kev (LECS) and 1 – 12 kev (MECS), with similar energy resolution; the data consists of photon arrival times tagged with $16\ \mu\text{s}$ precision. All data were pre-screened during the standard SAX pipeline processing to remove times of enhanced background resulting in usable exposure times of 57.9 ks for each of the MECSs and 26.5 ks for the LECS. Here we concentrate exclusively on photons obtained with the two MECS detectors, which makes up the bulk of the data. Data from the two MECS were merged and barycentered by the SAX team.

For all data sets we extracted barycenter corrected arrival times from a $\simeq 4'$ radius aperture centered on the central object in Kes 73 and restricted the energy range to 2 – 10 keV. We then searched these time series for coherent pulsation by folding the data about the expected periods derived from the ephemeris of VG97. In each case highly significant power is detected in the resulting periodograms corresponding to the central pulsar's pulse period at the specific epoch. Figure 1 compares periodograms of the *ASCA* data of 1993 and 1998 produced in the manner described above. We plot these on the same scale to emphasized both the significance of the detection and the unambiguous change in period between the two epochs.

2.2. Ginga & RXTE Datasets

With a period detection in hand, we re-analysed archival data from the *Ginga* (Makino 1987) and *RXTE* (Bradt et al. 1993) missions. The main instrument on-board *Ginga* is the non-imaging Large Area Counter (LAC) which covers an energy range of 1 – 37 kev with an effective area of $4000\ \text{cm}^2$ over its $\sim 2 \times 2$ field-of-view. *Ginga* observed Kes 73 twice in data modes with sufficient temporal resolution ($2\ \mu\text{s}$ or $16\ \mu\text{s}$ depending on data mode) and exposure to carry out the present analysis (see Table 1). These data were screened using the following criteria: i) Earth-limb elevation angle > 5 degrees ii) cut-off rigidity $> 8\ \text{GeV}/\text{c}$, and iii) South Atlantic Anomaly avoidance. The LAC light curves were restricted to the $\sim 1 – 17$ keV energy band-pass and corrected to the solar heliocenter using available software⁴

Kes 73 was observed for 5 ks by *RXTE* during 1996 as part of the GO program. We analyzed archive data acquired with the Proportional Counter Array (PCA) in “Good Xenon” data mode at $0.9\ \mu\text{s}$ time resolution. The PCA instrument is similar to the LAC, with a smaller field-of-view and a greater effective area of $6,500\ \text{cm}^2$. The two *RXTE* observation windows were scheduled so that no additional time filtering was required. After processing and

barycentering the Good Xenon data according to standard methods, we selected events from layer 1 only and applied an energy cut of $\lesssim 10\ \text{keV}$.

As found with the imaging data, epoch folding around the anticipated period produced a highly significant period detection. These periods are consistent with the extrapolated *ASCA* derived ephemeris. In Figure 2 we display pulse profiles of Kes 73 at two epochs separated by over a decade to look for possible long term changes. To improve the signal-to-noise in the latter observation, we have co-added phased aligned profiles from the 1998 *ASCA* and the 1999 *BeppoSAX* observations. No significant differences were found between the two pulse profiles, which are identical to the 1993 *ASCA* and 1996 *RXTE* profiles, to within statistical uncertainties.

2.3. 1E 1841–045: Timing Characteristics

In order to accurately determine the detected period at each epoch we oversampled the pulse signal by zero-padded the lightcurves (binned at 1 s resolution) to generate 2^{20} point FFTs. We then fit for the centroid to the peak signal to determine the best period. In none of the cases do we detect significant higher harmonics, a fact consistent with the roughly sinusoidal shape of the pulsar's profile.

To estimate the uncertainty in the period measurements we carried out extensive Monte-Carlo simulations. For each data set we generated a set of simulated time series whose periodicity, total count rate, and noise properties and observation gap are consistent with the actual data set for each epoch. We used the normalized profile folded into 10 bins, to compute the probability of a photon arriving in a given phase bin. Each realization of the simulated data was subjected to the same analysis as the actual data sets to obtain a period measurement. After 500 trials we accumulated a range of measured periods which was well represented by a normal distribution. The resulting standard deviation of this function is taken as the 1-sigma uncertainty in the period and is presented in table 1. The errors in the period are roughly consistent with the size of a period element divided by the signal-to-noise of each detection.

Each period measurement was assigned an epoch defined as the mid-observation time (in MJD) for that data set. The period measurements and their uncertainties were then fit with simple first-order and second-order models to evaluate the spindown characteristics. The parameters were P_s , \dot{P}_s with the addition of the second derivative \ddot{P}_s for the second order fit, with the spin history written as a Taylor expansion. The best fit to the linear model gives the following period ephemeris (Epoch MJD 49000), $P = 11.765732 \pm 0.000024\ \text{s}$; $\dot{P} = 4.133 \times 10^{-11} \pm 1.4 \times 10^{-13}\ \text{s s}^{-1}$.

The linear spindown model was consistent with the data with fit residuals at the $10^{-4}\ \text{s}$ (or 0.1 micro-Hz) level. We found that these residual were not sensitive to a second derivative of the period. An upper-limit allowed by the available datasets and their associated errors is more than an order-of-magnitude larger than expected just due to classic vacuum dipole spindown; for a vacuum dipole rotator one expects $\ddot{P}_s \simeq (2 - n)\dot{P}_s^2/P_s$; where $n = 3$ is the

⁴The barycentric correction to these periods is small and has been added in, along with the statistical error in the periods.

braking index in the vacuum dipole formalism.

3. DISCUSSION

In its observed characteristics, 1E 1841–045 most resembles the anomalous X-ray pulsars (AXPs), with its slow, ~ 10 s pulse period, steep X-ray spectral signature, inferred luminosity of $\sim 4 \times 10^{35}$ erg s $^{-1}$ cm $^{-2}$, and lack of counterpart at any wavelength. It is, however, unique among these objects in its apparent temporal and spectral stability. The two AXPs for which sufficient monitoring data is available, 2259+586 and 1E 1048–59, show large excursions in flux ($\gtrsim 3$) and significant irregularities in their spin down ($\log(|\delta P/P|) \sim -4$). Compared with these objects, the spindown of 1E 1841–045 suggests a lower level of torque fluctuations. For 1E 1841–045, the magnitude of timing irregularities, given by the timing residuals after subtracting the linear model, is $\log(|\sigma/P|) < -5$, where $\sigma \sim 10^{-4}$ s is the typical size of the measurement error (Table 1). The spindown of this object is apparently quieter than that observed in some middle-aged pulsars, which have red noise fluctuations in the pulse times-of-arrival of order -3 to -4 (e.g. Arzoumanian et al. 1994).

There is mounting evidence that, as a class, AXPs are related to the soft γ -ray repeaters (SGR), given their similar X-ray spectral and timing properties. If the spindown were to show systematic departures from linearity as in the case of glitches, which might be accompanied by bursting activity (as is the case in the SGRs, and may be expected in 1E 1841–045 if it is ultramagnetized), then such activity has so-far not been detected by orbiting γ -ray observatories, nor is it reflected in the spin history. Note that the glitch observed from SGR 1900+14 resulted in a period change an order of magnitude larger, $\log(|\delta P/P|) \simeq -4.3$ (Kouveliotou et al. 1999).

In the context of an evolutionary link between the SGRs and AXPs, the timing and spectral stability of 1E 1841–045 suggest a quiescent state either pre- or post-SGR activity. The relative age of 1E 1841–045 argues for an early state, possibly preceding γ -ray activity, as there is some evidence that 1E 1841–045 is the youngest amongst the currently recognized AXPs and SGRs. Half the AXPs are known to be associated with supernova remnants, while of the four known soft repeaters - two have host remnants while another, SGR 1806–20, has associated plerion-like emission but no discernible supernova shell. All these objects are thought to be at least $\gtrsim 10^4$ yr-old, with the oldest AXPs having been around for a few $\times 10^5$ years (spindown on timescales of a few hundred years observed in SGRs is no reflection of their true ages).

Rotational energy loss is insufficient to power the inferred luminosity of 1E 1841–045, unlike in the usual radio pulsar. In the SGRs, the ultimate mechanism for powering particle acceleration is naturally the release of magnetic free energy (both steady and episodic-seismic), rather than rotation. The episodic emission of γ -ray bursts is thought to be due to starquakes in the neutron star crust. This could suggest a future “turning-on” of 1E 1841–045 as a γ -ray repeater on several thousand year timescale, presumably resulting from a slow buildup of stress between the core and surface of the neutron star due to, a yet, unknown state transition in the stellar crust.

The blackbody spectrum suggests a radiating surface of size $R_\infty \simeq 8d_7^2$ km, were d_7 is the distance to Kes 73 in

units of 7 kpc, which is consistent with neutron stellar dimensions (assuming an isotropic emitter and ignored surface redshift and photospheric corrections to the observed spectral energy distribution). This rough estimate suggests low surface temperature anisotropies (as opposed to small hotspots), and is in agreement with the low modulation, broad pulse originating from near the stellar surface. In an ultramagnetized neutron star, outward energy transport from a decaying magnetic field can keep the surface at elevated temperatures, with high thermal luminosities ($\sim 10^{35}$ erg s $^{-1}$), not observed normal neutron stars at age $\sim 10^3$ yr. In contrast, researchers have argued (Heyl & Hernquist 1998) that the X-ray luminosities in such stars may be driven by the cooling of the neutron star through a strongly magnetized, light-element envelope without the need for appreciable field decay (see also Heyl & Kulkarni 1999). Along with these cooling emissions from the surface, the star may have a magnetically-driven, charged-particle outflow as is suggested by VLA observations of the SGR 1806–20 (Frail, Vasisht & Kulkarni 1997) via the energetics and small scale structure of its plerion. Evidence a more episodic particle ejection, rather than a steady wind, is inferred from the recent radio flare observations of SGR 1900+14, taken during a period of high activity (Frail, Kulkarni & Bloom 1999).

For 1E 1841–045, we can only attempt to place limits on a steady pair-wind luminosity: upper limits to radio emission from a putative plerionic structure surrounding the pulsar, suggest an averaged pair luminosity of less than 10^{36} erg s $^{-1}$. Similarly, limits on a hard X-ray tail suggest a present day wind luminosity to be less than 5×10^{35} erg s $^{-1}$; the latter condition assumes a tail with a photon index of 2, quite typical of plerions, and a soft X-ray radiation conversion efficiency of 10 percent. This bounds are well within the energy budget available from field decay,

$$L_B \simeq (1/6)\dot{B}BR^3,$$

which is expected to power a bolometric luminosity of $\lesssim 10^{36}$ erg s $^{-1}$; the fastest avenue for stellar field decay would be the modes of ambipolar diffusion for which theoretical arguments suggest a timescale of decay (B/\dot{B}) of $\sim 3B_{15}^2$ kyr (Goldreich & Reisenegger 1992). Note that these upper limits are a factor $\sim 10^2$ larger than the star’s dipole luminosity of $4\pi^2 I\dot{P}/P^3 \sim 10^{33}$ erg s $^{-1}$. This suggests that spindown torques on the star could conceivably be dominated by wind torques, although such a wind would have to be remarkably steady to not produce timing residuals larger than those observed (Thompson & Blaes 1998). Alternatively, if classical dipole radiations is the primary spindown mechanism, then the stellar magnetic field is $B \simeq 0.75B_{15}$ G.

To conclude, ongoing X-ray timing monitoring of the spin period is underway by independent groups, including ours, which will provide accurate measurement of the braking index of this pulsar. As previously mentioned, a large braking index may directly reflect on active field decay or field re-alignment inside the the star. The observed braking index in a pure dipole rotator with loss of torque due to field decay may be written as

$$n_{obv} = 3 - 2\left(\frac{P}{\dot{P}}\right)\left(\frac{\dot{B}}{B}\right).$$

Given that the spindown timescale for this pulsar is about 9 kyr, a field decay time of about $\lesssim 3B_{15}^2$ kyr could impose a fairly large curvature on the spindown. Perversely, the situation may be far more complicated with different factors such as dipole radiation, winds driven by magnetic activity, and field decay all competing for torque evolution. This, however, remains to be tested through accurate longterm timing. Measuring the pulsar spin via a series of

closely spaced observations may also reveal a wealth of information on possible glitching and the subsequent recovery by the star.

Acknowledgments: EVG is indebted to Jules Halpern and Daniel Q. Wang for discussions and insights into timing noise and measurement error. We thank Angela Malizia for barycentering our *BeppoSAX* data. This research is supported by the NASA LTSA grant NAG5-22250.

REFERENCES

Arzoumanian, Z., Nice, D. J., Taylor, J. H., & Thorsett, S. E. 1994, *ApJ*, 325
 Boella, G., Butler, R. C., Perola, G. C., Pero, L., Scarsi, L. & Bleeker, J. A. M. 1997, *A&ASS*, 122, 299
 Bradt, H. V., Rothschild, R. E. & Swank, J. H. 1993, *A&AS*, 97, 355.
 Corbet, R. H. D., Smale, A. P., Ozaki, M., Koyama, K. & Iwazawa, K. 1995, *ApJ*, 443, 786
 Cordes, J. M. & Helfand, D. J. 1980, *ApJ*, 239, 640
 Frail, D. A., Kulkarni, S. R. & Bloom, J. S. 1999, *Nature*, in press; [astro-ph/981245](http://arxiv.org/abs/astro-ph/981245)
 Frail, D. A., Vasisht, G. & Kulkarni, S. R. 1997, *ApJ*, 480, L129
 Ghosh, P., Angelini, L. & White, N. E. 1997, *ApJ*, 478, 713
 Goldreich, P. & Reisenegger, A. 1992, *ApJ*, 395, 250
 Gotthelf, E. V. & Vasisht, G. 1997, *ApJ*, 486, L129
 Helfand, D. J., Becker, R. H. & White, R. L. 1994, *ApJ*, 434, 627
 Heyl, J. S. & Hernquist, L. 1998, *MNRAS*, 297, L69
 Heyl, J. S. & Kulkarni, S. R. 1998, *ApJ*, 506, L61
 Kriss, G. A., Becker, R. H., Helfand, D. J. & Canizares, C. J. 1985, *ApJ*, 288, 703
 Kouveliotou, C. et al. 1998, *Nature*, 391, 235
 Kouveliotou, C., Strohmayer, T., Hurley, K., van Paradijs, J., Dieters, S., Woods, P., Thompson, C. & Duncan, R.C., 1999, [astro-ph/9809140](http://arxiv.org/abs/astro-ph/9809140)
 Makino, F. et al. 1987, *Astrophys. Letters Commun.* 25, 223
 Mereghetti, S. & Stella, L. 1995, *ApJ*, 442, L17
 Sanbonmatsu, K. Y. & Helfand, D. J. 1992, *AJ*, 104, 2189
 Parmar, A. N. et al. 1997, *A&A*, 323, L29
 Tanaka, Y., Inoue, H. & Holt, S. S. 1994, *PASJ*, 46(3), L37
 Thompson, C. & Blaes, O. 1998, *Phys. Rev. D*, 57, 3219
 van Paradijs, J., Taam, R. E. & van den Heuvel, E. P. J. 1995, *A&A* 299, L41
 Vasisht, G. & Gotthelf, E. V. 1997, *ApJ*, 486, L129 (VG97)

TABLE 1
 OBSERVATION LOG FOR THE KES 73 PULSAR

Start Date UT	Mission	Exposure (ks)	Epoch ^a (MJD)	Period (s)	Uncert. ^b (μ s)
08 May 1987 06:28	<i>Ginga</i>	37.6	46924.5142361	11.758320	7
24 Apr 1991 17:27	<i>Ginga</i>	11.6	48371.2447166	11.76346	23
16 Mar 1992 04:30	<i>ROSAT</i>	25.1	48698.1946593	11.7645	...
11 Oct 1993 14:56	<i>ASCA</i>	39.6	49272.0820309	11.76676	45
31 Aug 1996 14:21	<i>RXTE</i>	5.9	50326.6953400	11.7707	375
27 Mar 1998 22:30	<i>ASCA</i>	38.7	50900.4509668	11.77248	50
08 Apr 1999 03:41	<i>BeppoSAX</i>	57.8	51276.8889120	11.77387	34

^aEpochs are given for the mid-observation, with time in MJD.

^bPeriod uncertainties quoted as 1σ ; see text for method.

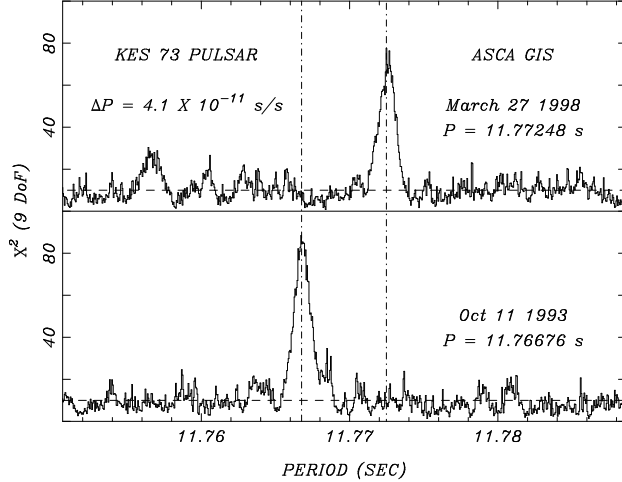


FIG. 1.— The *ASCA* detections of the Kes 73 pulsar at two epochs. These periodograms depict χ^2 of the light curve folded into 10 phase bins tested against a null-hypothesis as a function of trial fold periods. (Lower panel) The original discovery detection of Oct 11 1993 GIS and (Upper panel) the follow-up March 27 1998 GO observation. The change in period is highly significant and clearly resolvable; the period derivative, assuming a linear trend, is $\simeq 4.1 \times 10^{-11}$ s/s. The dashed horizontal lines represent the expected 1σ noise levels.

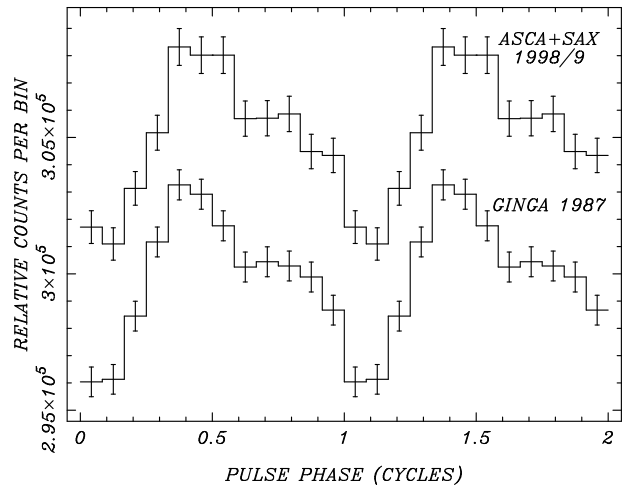


FIG. 2.— The pulse profiles of the Kes 73 pulsar at two epochs aligned in phase. The 1987 *Ginga* data (Bottom), and the 1998 *ASCA* and 1999 *BeppoSAX* data (Top) phased and co-added to give increased signal-to-noise. An invariant, Bactrian camel-like profile is observed in both cases. Two cycles are shown for clarity.

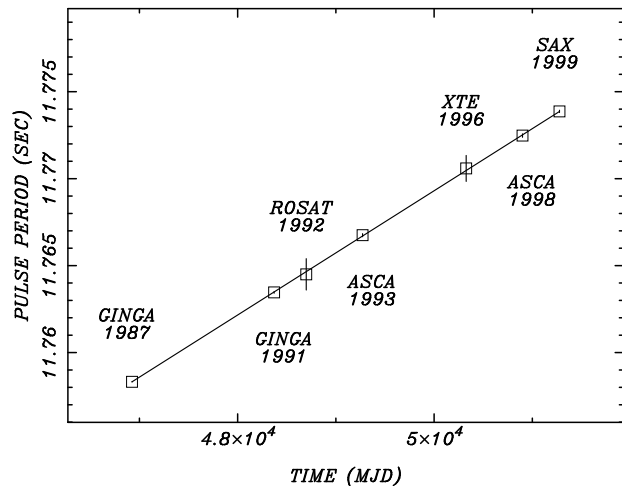


FIG. 3.— The long-term spin-down history of the Kes 73 pulsar. The square markers denote the spin period versus epoch; the solid line follows the best fit linear model (model parameters in section 2) The data points are depicted with 1σ error bars.